Macromolecules
ARTICLE

Macromolecules **2010**, *43*, 4991–4999 **4991**
DOI: 10.1021/ma100662x

Blends of Paclitaxel with POSS-Based Biodegradable Polyurethanes: Morphology, Miscibility, and Specific Interactions

Qiongyu Guo,[†,‡] Pamela T. Knight,[†,‡] Jian Wu,[‡,§] and Patrick T. Mather*[,‡,§]

[†]*Department of Macromolecular Science and Engineering, Case Western Reserve University, 2100 Adelbert Road, Cleveland, Ohio 44106,* [‡]*Syracuse Biomaterials Institute, and* [§]*Department of Biomedical and Chemical Engineering, Syracuse University, Syracuse, New York 13244*

Received March 27, 2010; Revised Manuscript Received May 7, 2010

ABSTRACT: The morphology, miscibility, and specific interactions of paclitaxel (PTx) with a family of polyhedral oligosilsesquioxane (POSS)-based biodegradable thermoplastic polyurethanes (POSS TPUs) were investigated systematically using wide-angle X-ray diffraction (WAXD), differential scanning calorimetry (DSC), and Fourier transform infrared spectroscopy (FTIR). These POSS TPUs incorporate an alternating multiblock structure formed by POSS hard segments and the soft segments composed of polylactide/caprolactone copolymer (P(DLLA-*co*-CL)). They feature variable poly(ethylene glycol) (PEG) content from 0 to 14 wt % through adjusting the poly(ethylene glycol) (PEG) molecular weight in P(DLLA-*co*-CL) soft segments of fixed molar mass of $\bar{M}_n$ = 12 kg/mol and further to 52 wt % utilizing pure PEG $\bar{M}_n$ = 1 kg/mol in the soft segments. Using WAXD, it was found that PTx is amorphous in all proportions in the PTx/POSS TPU blends prepared using a solution-casting method. Interestingly, the PTx not only exhibits excellent miscibility in all of these PTx/POSS TPU blends over the whole range of the drug concentration, but also serves as an antiplasticizer by increasing the blend T_g gradually from the polymer T_g up to the T_g of amorphous PTx. The T_g−composition dependences in these blends were well fitted by the Gordon−Taylor equation. The glass transition breadth of the blends increases significantly only for drug concentrations higher than 50 wt % for most of the POSS TPUs, suggesting some spatial heterogeneity at these high drug concentrations. On the other hand, the slight increment of the blend melting temperature, T_m, and latent heat, ΔH, indicates enhanced phase separation between the POSS hard segments and the TPU soft segments upon drug incorporation. Gordon−Taylor analysis and FTIR results confirm that the PEG incorporated in the POSS TPUs exhibits strong H-bonding interactions with the PTx. Although PEG can promote the favorable interactions in the PTx/POSS TPU blends, we showed that the more hydrophobic LA/CL repeat units are still required in the soft segments in order to achieve molecular-level miscibility. This systematic investigation of the PTx/POSS TPU systems may be of great value to design plasticizer/antiplasticizer for new polymer materials with controlled and tailored properties, especially for those PLA- or PCL-based biodegradable polymer systems.

Introduction

Molecular miscibility of drugs, especially those of poor water solubility, in polymeric drug-delivery systems is highly desirable to achieve high drug bioavailability and controlled drug-release kinetics.[1−3] Ideally, the drugs in such systems are amorphous and can serve as either an antiplasticizer or a plasticizer when their glass transition temperatures, T_gs, are higher or lower than the polymers, respectively. Here we call a small molecular drug additive as antiplasticizer when the incorporation of the additive into the polymers leads to an increase of the T_g, causing a reduction of polymer segmental mobility and an enhancement of polymer stiffness. As is known, paclitaxel (PTx) is an anticancer therapeutic agent widely adopted for the clinical treatment of various human cancers,[4] and has also been successfully administered in Taxus drug-eluting stents (Boston Scientific Corp., Natick, MA) for the treatment of in-stent restenosis.[5] Nevertheless, the therapeutic efficacy of this drug has been hampered by its extremely low water solubility of ∼1 μg/mL.[6,7] In order to enhance its aqueous solubility and/or achieve controlled/targeted release, a great many polymeric formulations of paclitaxel have been developed, including coatings,[8−10] liposomes,[11−13] micelles,[14−16] and micrometer- and nano-size particles.[17−19] In these polymeric formulations, most studies have found that the paclitaxel was amorphous at low concentrations in the polymers. Lee et al.[16] investigated the solubilization of paclitaxel into hydrotropic polymeric micelles using diblock copolymers of poly(ethylene glycol) and poly(2-(4-vinylbenzyloxy)-*N*,*N*-diethylnicotinamide). They observed no melting endotherm of paclitaxel in thermal analysis of the polymeric micelles even at a high drug loading of 31.7 wt %, indicating that the drug existed in an amorphous state. Zhang et al. reported that paclitaxel was amorphous in the poly(DL-lactide)-*block*-methoxy poly(ethylene glycol) (PDLLA-*b*-MePEG) matrix at a drug loading of 10 wt % prepared using solution-casting method, but showed crystalline peaks in the powder X-ray diffraction patterns in the blend at the same drug loading obtained using the melt mixing method.[20] The SEM results of Dhanikula et al. clearly exhibited fibrous, recrystallized paclitaxel on the surface of chitosan films with a drug loading of 31 wt %.[21]

Despite these findings, very few systematic works have been published concerning the molecular miscibility of paclitaxel in the solid-state polymeric formulations. The glass transition temperature (T_g) of amorphous paclitaxel is reported to be around 150 °C,[6,22] much higher than those of most drug-delivery polymers. Therefore, it is expected that the amorphous paclitaxel will act as an antiplasticizer and enhance the T_g of molecularly miscible polymeric formulations when the pure polymer T_g is lower than the drug T_g. Cho et al.[8] and Richard et al.[23] observed a continuous increment of T_g with increasing paclitaxel concentration

*To whom correspondence should be addressed. E-mail: ptmather@syr.edu.

Published on Web 05/14/2010

up to 25 wt % in their block copolymers and concluded that the drug was at least partially miscible with the polymers. In contrast, Westedt et al. showed an inverse dependence of the blend T_g on the paclitaxel concentration in the films of poly(vinyl alcohol)-*graft*-poly(lactic-*co*-glycolic acid) (PVA-*g*-PLGA).[24] This can probably be attributed to the poor miscibility of paclitaxel with the polymer since they reported that paclitaxel crystals appeared starting from a low drug loading of 10 wt %. The increase of T_g due to the antiplasticization effect has also been sparsely reported in the polymeric systems for other drugs. For instance, Lionzo et al. observed a slight increment of the glass transition temperature of poly(hydroxybutyrate-*co*-hydroxyvalerate) in the dexamethasone acetate-loaded microparticles compared to the raw polymers.[25] Chokshi et al. reported the antiplasticization effect of indomethacin in Eudragit EPO, an aminoalkyl methacrylate copolymer, for various binary mixtures.[26]

Paclitaxel/polymer interactions may play a critical role in the miscibility and distribution of the drug in the polymers. Richard et al. reported that paclitaxel preferentially resides in the poly(*n*-butyl acrylate) (PBA) phase of poly(methyl methacrylate-block-*n*-butyl acrylate-*block*-methyl methacrylate) (PMMA-*b*-PBA-*b*-PMMA)) triblock copolymers.[23] In contrast, Cho et al. found that the paclitaxel segregated to the PMMA phase in the triblock copolymer of poly(methyl methacrylate-*b*-isobutylene-*b*-methyl methacrylate) (PMMA-*b*-PIB-*b*-PMMA).[8] The apparent discrepancy between these findings confirms the importance of the interactions between the paclitaxel and different blocks in controlling drug distribution. Recently, Kang et al. investigated the paclitaxel distribution in PLGA/PEG blends by selectively imaging the three components using coherent anti-Stokes Raman scattering (CARS) microscopy.[27] In the 9:1 and 8:2 PLGA/PEG films, they not only observed that paclitaxel preferentially partitioned into the PEG domains in the blends, but also found that the strong interactions between paclitaxel and PEG prevented the crystallization of PEG. Moreover, they observed a uniform mixing of paclitaxel in both PLGA and PEG in PLGA/PEG (7:3) films.

In this study, we systematically probe the morphology, miscibility, and specific interactions of paclitaxel over all proportions of the drug concentrations in a family of polyhedral oligosilsesquioxane (POSS)-based biodegradable thermoplastic polyurethanes (TPU) synthesized in our group.[28] These POSS TPUs feature alternating multiblock structures of hard segments containing nonbiodegradable POSS and biodegradable soft segments. The POSS hard segments aggregate to form crystals serving as physical cross-links on the nanometer scale. The biodegradable soft segments are amorphous polylactide/caprolactone copolymer (P(DLLA-*co*-CL)) incorporating PEG covalently. We mainly modulate the PEG content and the copolymer composition in the soft segments of these polyurethanes, which leads to varying polyurethane T_g from 49 to −42 °C. Previously, we reported highly adjustable and precisely controllable release of paclitaxel from these polymers.[10] Here, we employ wide-angle X-ray diffraction (WAXD) to determine the crystalline/amorphous morphology of the paclitaxel in the PTx/POSS TPU blends prepared using a solution-casting method, employ differential scanning calorimetry (DSC) to monitor the influence of the incorporation of the paclitaxel on the thermal behavior of the PTx/POSS TPU blends, and utilize Fourier transform infrared spectroscopy (FTIR) to ascertain the specific interactions, especially hydrogen-bonding interaction, between the drug and the polymers. In doing so, we reveal the dependence of morphology, miscibility, and specific interactions of the blends on PEG content.

Experimental Section

Materials. Paclitaxel was kindly provided by Boston Scientific Corp. (Natick, MA) (Scheme 1). Tetrahydrofuran (THF) (histological grade) was purchased from Fisher and used as received. The POSS TPUs were synthesized as described earlier.[10,28] A naming system of these polymers designed before[10] is utilized in this study. Totally, five POSS TPUs were selected. They are $[B\_LA_{100}CL_0]$-$[LP]_3$, $[P_{1k}LA_{100}CL_0]$-$[LP]_3$, $[P_{1k}LA_{90}CL_{10}]$-$[LP]_3$, $[P_{2k}LA_{100}CL_0]$-$[LP]_3$, and $[P_{1k}LA_0CL_0]$-$[LP]_{0.8}$ (Table 1 and Scheme 2). As shown, the names of the POSS TPUs include two parts. The first part contains the compositional information on the polyol soft segment, while the second part indicates the polyurethane synthesis information. For example, $[B\_LA_{100}CL_0]$-$[LP]_3$ uses the polyol initiated from 1,4-butanediol, containing 100% lactyl repeat units with no caprolactone. In the second part, L stands for diisocyanate of LDI, and P stands for POSS. The number 3 indicates that the feed ratio of POSS to polyol is three. Similarly, $[P_{1k}LA_{90}CL_{10}]$-$[LP]_3$ consisted of a P(DLLA-*co*-CL) soft segment prepared using an initiator of PEG $\bar{M}_n$ = 1 kg/mol instead of 1,4-butanediol, and molar feed ratio of LA to CL repeat units of 90:10.

Scheme 1. Chemical Structure of Paclitaxel

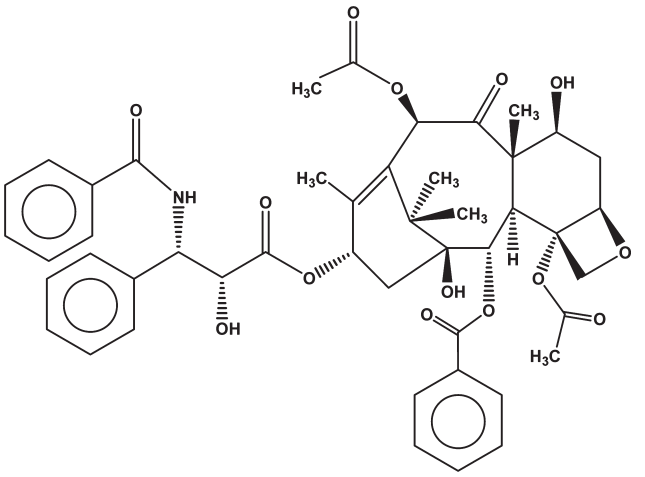

Sample Preparation. PTx/POSS TPU blends were first prepared to contain PTx concentrations from 0 to 100 wt % with increments of 10 wt %. They were cast from THF solutions (10% w/v) on Teflon casting dishes covered by aluminum foil to control the solvent evaporation rate. The films were dried in air at ambient condition for a few days, then under vacuum at room temperature (> 12 h), and finally under vacuum at about 70 °C (> 24 h). After the films were dried completely, they were stored in a desiccator for the following characterizations.

WAXD. The WAXD patterns of the films of PTx/POSS TPU blends were obtained using a Rigaku S-Max3000 (Woodlands, TX) in transmission mode. A Rigaku generator (MicroMax-002$^+$) was employed to produce a Cu Kα radiation with the wavelength of 1.5405 Å. An accelerating voltage of 45 kV and a current of 0.88 mA were applied. All samples were sandwiched between two layers of Scotch tape, and exposure times of 30 min were utilized. The two-layer tape was also tested and used as baseline. The WAXD patterns were recorded on an image plate of 152 mm × 152 mm with the sample-to-plate distance of 150 mm and read using an image plate reader (Fujifilm FLA-7000) using pixel size of 100 μm^2. The isotropic WAXD patterns were averaged azimuthally with the image sampling density of 1000 points to produce 1D spectra using a SAXSGUI software (v2.01.02). All reported WAXD curves have been subtracted by the pure two-layer tape baseline.

DSC. DSC (Q100, TA Instruments, New Castle, DE) was used to determine the phase behavior and thermal transitions of the films of PTx/POSSTPU blends. The film samples were the same as those for WAXD characterizations mentioned above. Each sample of ~3 mg was sealed in a TA aluminum pan. The DSC tests were performed by heating−cooling−heating between −90 and 180 °C at 10 °C/min under flowing nitrogen gas of 50 mL/min. The second heating traces, having all thermal

Table 1. Physicochemical Properties of POSS TPUs

POSS TPU	$\bar{M}_n$ (g/mol)/PDI	POSS ratio[a]	wt % POSS	wt % PEG	CL (%)[b]	T_g (°C)	T_m (°C) (ΔH, J/g)	POSS crystallinity (%)[c]	K_{fit}[d]
$[B\_LA_{100}CL_0]$-$[LP]_3$	49800/1.44	2.7	24	0	0	49	123 (0.93)	15	0.27
$[P_{1k}LA_{100}CL_0]$-$[LP]_3$	94800/1.30	2.6	24	6.8	0	36	113 (1.62)	26	0.37
$[P_{1k}LA_{90}CL_{10}]$-$[LP]_3$	51900/1.50	2.7	24	6.7	13	18	124 (1.88)	30	0.41
$[P_{2k}LA_{100}CL_0]$-$[LP]_3$	68800/1.52	2.4	22	13.8	0	25	121 (1.71)	30	0.44
$[P_{1k}LA_0CL_0]$-$[LP]_{0.8}$	127000/1.21	0.57	48	51.8	0	−42	121 (5.79)	47	0.59

[a] Actual ratio as determined by ^{1}H NMR. [b] mol % CL in polyol as determined by ^{1}H NMR. [c] Determined by [ΔH (J/g)/ (25.91 J/g × wt %POSS)] × 100%, where 25.91 J/g is the heat of fusion of the POSS diol monomer. [d] Fitted using Gordon−Taylor equation, eq 1.

Scheme 2. General Structure of the POSS TPUs and Their Different Polyols (〰) Used To Create a Variety of Polyurethane Compositions

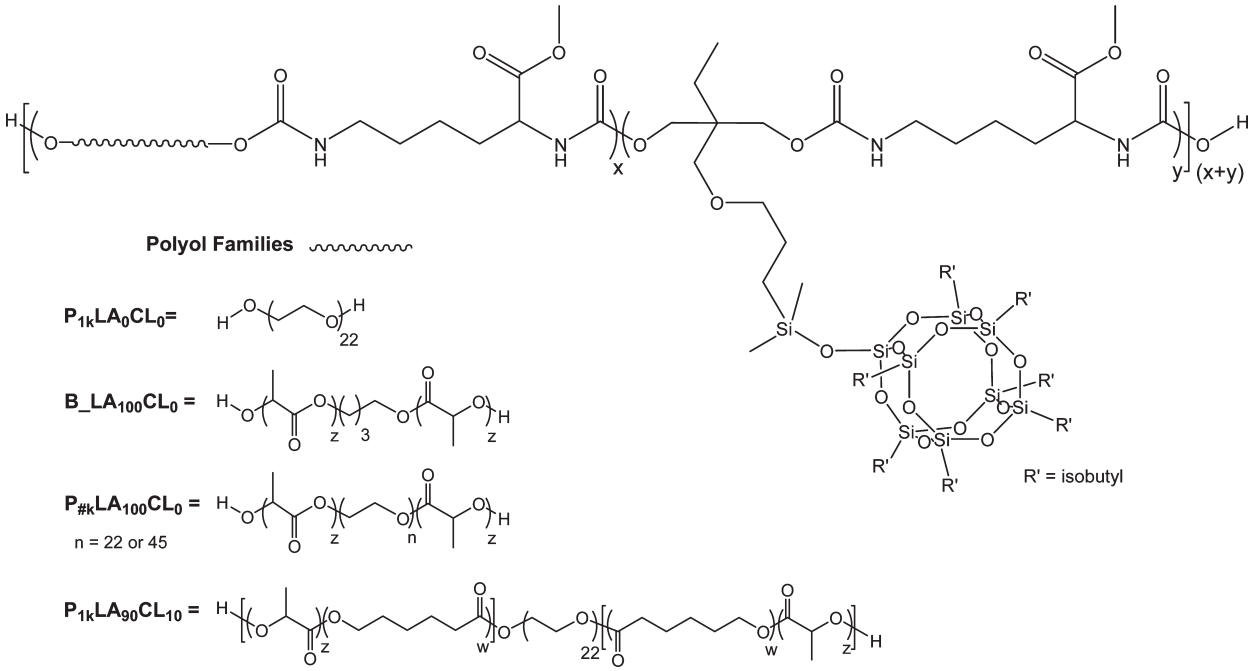

history erased, were analyzed by Universal Analysis 2000 software (TA Instruments) to determine the glass transition temperature (T_g), glass transition breadth, the melting temperature (T_m), and the heat-of-fusion (ΔH). T_g was obtained as the temperature at the half height from the onset to the end of the stepwise decrease of the heat flow trace. Glass transition breadth, which will be further discussed in the Results and Discussion, was determined from the derivative heat flow smoothed using a smoothing region width of 5 °C by Universal Analysis 2000 software. T_m was the temperature at the valley (most negative value) of the endothermic peak. ΔH was measured through integration of the peak and normalization by the sample mass.

FTIR. The FTIR measurements of the PTx/POSS TPU blends were performed on a Perkin-Elmer Spectrum One FTIR spectrometer (Waltham, MA). The blend specimens for FTIR were prepared using following procedures. Two or three drops of the THF solutions (10% w/v) of the PTx/POSS TPU blends with various PTx concentrations were placed onto KBr windows (25 mm in diameter × 2 mm in thickness), dried in air for half an hour, then dried in a vacuum oven at 100 °C for 3 h, and finally cooled down in a desiccator at room temperature for at least half an hour. In this way, very thin dried coatings were prepared on the KBr windows for FTIR tests. The FTIR spectra were averaged for 20 scans at a resolution of 1 cm^{-1}.

Results and Discussion

Five POSS TPUs with varying PEG content were employed to form the blends with paclitaxel (Table 1). The percentage of PEG incorporated in the POSS TPUs increases from 0 wt % for $[B\_LA_{100}CL_0]$-$[LP]_3$, to 7 wt % for $[P_{1k}LA_{100}CL_0]$-$[LP]_3$ and $[P_{1k}LA_{90}CL_{10}]$-$[LP]_3$, to 14 wt % for $[P_{2k}LA_{100}CL_0]$-$[LP]_3$, to finally 52 wt % for $[P_{1k}LA_0CL_0]$-$[LP]_{0.8}$. Among these POSS TPUs, $[P_{1k}LA_0CL_0]$-$[LP]_{0.8}$ is unique in that its soft segment contains purely PEG of $\bar{M}_n$ = 1 kg/mol and its POSS:polyol feed mole ratio is 0.8. All of the other four POSS TPUs were synthesized using the PDLLA or P(DLLA-*co*-CL) polyol segments with a total molecular weight (including initiator) of 12 kg/mol with POSS:polyol feed mole ratio of 3. The initiators used for the polyol segments of $[B\_LA_{100}CL_0]$-$[LP]_3$, $[P_{1k}LA_{100}CL_0]$-$[LP]_3$ and $[P_{2k}LA_{100}CL_0]$-$[LP]_3$ are 1,4-butanediol, PEG $\bar{M}_n$ = 1 kg/mol and PEG $\bar{M}_n$ = 2 kg/mol, respectively. Compared to $[P_{1k}LA_{100}CL_0]$-$[LP]_3$, $[P_{1k}LA_{90}CL_{10}]$-$[LP]_3$ employed the same initiator in the polyol segment but consisted of LA to CL repeat units of 90:10 in the feed mole ratio instead of pure LA.

Morphology. *Polymer Morphology*. The nature of the crystalline/amorphous morphology of the POSS TPUs, comparing with that of the POSS diol monomer, was examined using WAXD. The crystallization patterns of the POSS diol monomer and $[P_{1k}LA_{100}CL_0]$-$[LP]_3$ have been previously described in some detail.[28,29] Similar to these prior results, as shown in Figure 1, the POSS diol monomer exhibits three strong characteristic diffraction peaks at scattering angles of 2θ = 7.9°, 10.7°, and 19.3°, corresponding to *d*-spacing values of 11.18, 8.24, and 4.61 Å, respectively. The incorporation of POSS in the $[P_{1k}LA_{100}CL_0]$-$[LP]_3$ uniformly shifts the three POSS characteristic peaks to higher angles at 2θ = 8.3°, 11.1°, and 19.9°, which correspond to smaller *d*-spacing values of 10.67, 7.93, and 4.45 Å, respectively. Despite variation in polyurethane composition, all of

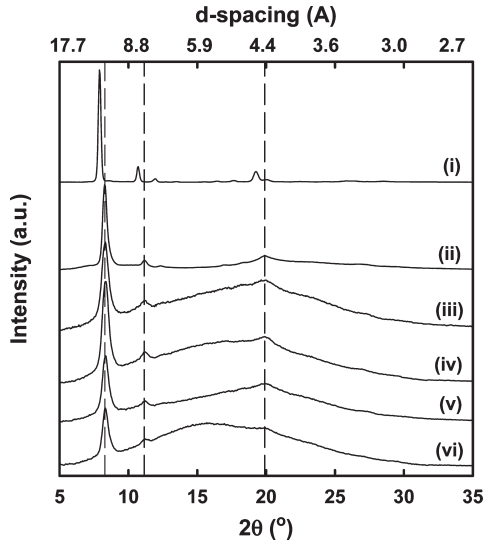

Figure 1. WAXD of (i) POSS diol monomer, (ii) $[P_{1k}LA_0CL_0]$-$[LP]_{0.8}$, (iii) $[P_{2k}LA_{100}CL_0]$-$[LP]_3$, (iv) $[P_{1k}LA_{100}CL_0]$-$[LP]_3$, (v) $[P_{1k}LA_{90}CL_{10}]$-$[LP]_3$, and (vi) $[B\_LA_{100}CL_0]$-$[LP]_3$.

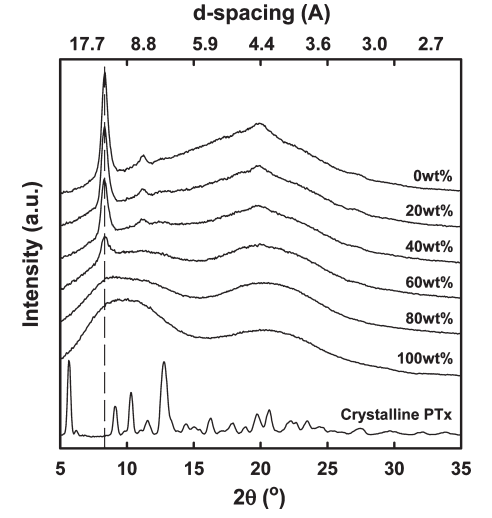

Figure 2. WAXD of crystalline paclitaxel and PTx/$[P_{1k}LA_{90}CL_{10}]$-$[LP]_3$ blends with the paclitaxel weight percentage indicated above each curve.

the other four POSS TPUs selected in this work exhibited the same scattering peaks as $[P_{1k}LA_{100}CL_0]$-$[LP]_3$. Further, an amorphous halo is also observed in all the POSS TPUs, especially for those with comparably low POSS content from 22 to 24 wt % (Table 1). The amorphous halo of $[B\_LA_{100}CL_0]$-$[LP]_3$ is comparably stronger than the other POSS TPUs (Figure 1) due to its lowest POSS crystallinity among the five polymers (Table 1). It is reasoned that the PEG incorporated in the other POSS TPUs enhanced the phase separation of the POSS hard segment from the TPU soft segments and so increased their POSS crystallinities. No additional scattering peaks can be found in the WAXD profiles, indicating that only the POSS in the polyurethanes forms crystals and that the polymer soft segments are amorphous.

PTx/POSS TPU Blends Morphology. The WAXD spectra of the PTx/POSS TPU blends with paclitaxel concentrations incremented by 20 wt % for all proportions were obtained and compared. As shown in Figure 2, the incorporation of the paclitaxel in $[P_{1k}LA_{90}CL_{10}]$-$[LP]_3$ only decreases the intensity of the POSS characteristic peaks. In addition, no new peaks can be found in all of the WAXD spectra of the blends. Similar results as $[P_{1k}LA_{90}CL_{10}]$-$[LP]_3$ were also observed for all the other four POSS TPUs (see Supporting Information for WAXD results). In contrast, the crystalline paclitaxel as received shows several strong X-ray diffraction peaks at 2θ from 5° to 25°, which is consistent with the previous reports.[6,20] Consequently, these results indicate that the paclitaxel is amorphous in the PTx/POSS TPU blends over the whole concentration range. We note that the pure paclitaxel prepared from the same solution-casting method as the PTx/POSS TPU blends (Figure 2, 100 wt %) is amorphous, also showing no crystalline peaks. As the paclitaxel concentration was increased, the peak of $2\theta = 8.3°$ characteristic for POSS crystal diminishes and finally disappears at the paclitaxel concentration of 80 wt % for all five POSS TPUs. Thus, at least 5 wt % POSS in all the POSS TPU blends is required to sustain the POSS crystallization, which plays a central role in maintaining the excellent mechanical properties of the polymer systems. We observed that the PTx/POSS TPU blends showing POSS crystallization produced mechanically strong transparent films following the solution-casting method. It was very difficult to obtain an intact film from those blends without significant POSS crystallization. A corroborating result was also observed in the POSS melting behavior using DSC second heating and will be discussed later.

Miscibility. The dependences of both the T_g and T_g breadth of the PTx/POSS TPU blends on PTx content were utilized to probe the miscibility of the paclitaxel with the POSS TPUs. Generally, the existence of a single glass transition without significant broadening indicates molecular miscibility between the blend components in an amorphous state.[30] In Figure 3a, we present the DSC second heating curves of PTx/$[P_{1k}LA_{90}CL_{10}]$-$[LP]_3$ blends to reveal the effect of the incorporation of paclitaxel in the thermal properties of the blends. In these DSC heating traces, only single T_gs were observed and the blend T_g increased gradually from the POSS TPU T_g (i.e., 18 °C) up to the T_g of amorphous paclitaxel (i.e., 147 °C) with increasing paclitaxel concentration. The augmentation of the blend T_g upon incorporation of paclitaxel supports a hypothesis of an antiplasticization effect of the drug and indicates excellent miscibility between paclitaxel and $[P_{1k}LA_{90}CL_{10}]$-$[LP]_3$. Similar results were also observed for the blends of all the other POSS TPUs (see Supporting Information for DSC results). The excellent miscibility confirmed by DSC characterizations is consistent with our observation of the optical transparency of the PTx/POSS TPU cast films as mentioned above.

The composition dependence of the blend T_g was further analyzed using Gordon−Taylor equation.[31] The Gordon−Taylor equation is one of the most used expressions to describe the T_g−composition dependence of miscible polymer blends[30,32] and drug/polymer blends[33,34]

$$T_g = \frac{w_1 T_{g,1} + K w_2 T_{g,2}}{w_1 + K w_2} \quad (1)$$

where w_1 and w_2 are the weight fractions of the two components of the blend. Here we define the POSS TPU as component 1 and paclitaxel as component 2. The coefficient, K, is an adjustable parameter practically related to the degree of curvature of the T_g−composition curve. Great attention has been aroused recently to the correlation of the T_g−composition dependence to the dynamic properties of polymer blends using Lodge−McLeish model,[35−37] which is beyond the scope of our present study.

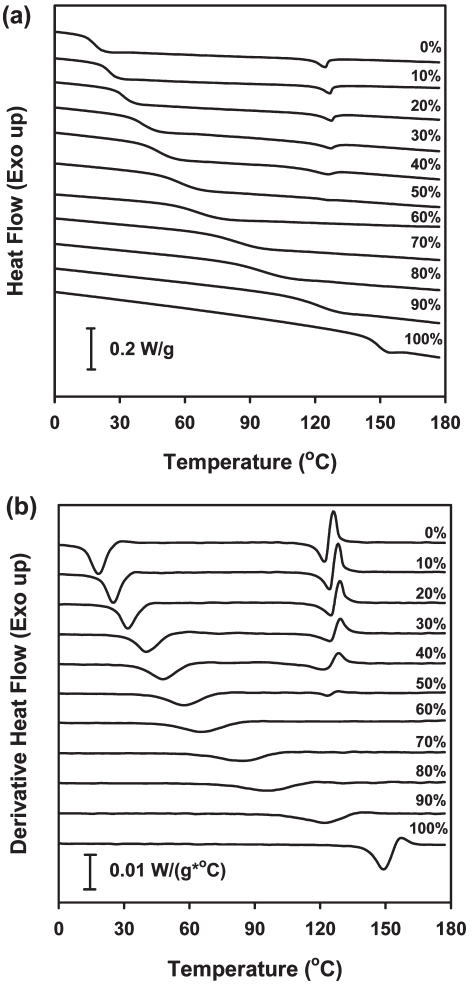

Figure 3. (a) DSC second heating curves and (b) corresponding derivatives of the DSC heating curves of PTx/$[P_{1k}LA_{90}CL_{10}]$-$[LP]_3$ blends with the paclitaxel weight percentage indicated above each curve. The heating rate was 10 °C/min.

Equation 1 assumes volume additivity in the blends, called the Gordon−Taylor volume additivity model,[38] for which K is determined by

$$K_{G-T} = \frac{\rho_1 \Delta\alpha_2}{\rho_2 \Delta\alpha_1} \quad (2)$$

where ρ_i and $\Delta\alpha_i = (\alpha_{melt} - \alpha_{glass})_{T_{g,i}}$ are the density and the increment of expansion coefficient at T_g of the component i, respectively. Assuming the validity of the Simha−Boyer rule[39] relating $\Delta\alpha$ and T_g

$$\Delta\alpha T_g \approx \text{constant}$$

Equation 2 can be rewritten as

$$K_{G-T} = \frac{\rho_1 T_{g,1}}{\rho_2 T_{g,2}} \quad (3)$$

As stated, this model assumes the ideal behavior of volume additivity and neglects potential influence of component interaction on K.

Figure 4 shows that the T_g−composition dependences of all PTx/POSS TPU blends were well fitted by the Gordon−Taylor equation. Since the densities of all POSS TPUs are close (1.3 g/cm^3 for $[P_{1k}LA_0CL_0]$-$[LP]_{0.8}$ and 1.2 g/cm^3 for the other POSS TPUs),[10] eq 3 can be simplified as

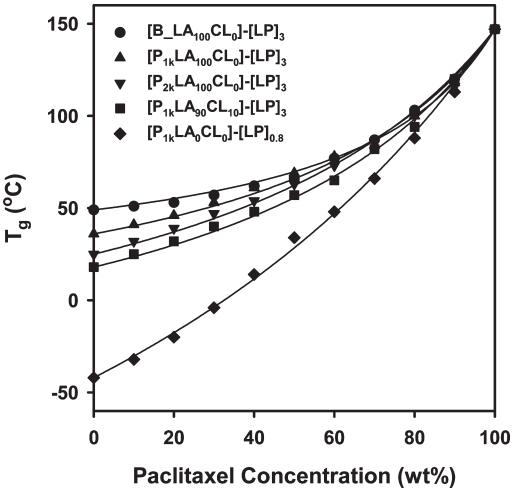

Figure 4. T_g vs paclitaxel concentration of the PTx/POSS TPU blends fitted by Gordon−Taylor equation with R^2 higher than 99.5% for all curves.

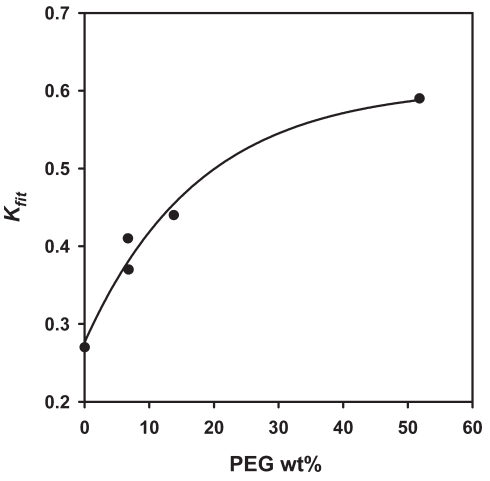

Figure 5. K_{fit} vs PEG content in POSS TPU. The curve is used to guide the trend of K_{fit} vs PEG content.

$$K_{G-T} \propto T_{g,\,\text{POSS TPU}} \quad (4)$$

According to eq 4 and considering the large range of the POSS TPU T_g from −42 to 49 °C, the K_{G-T} should increase greatly with the POSS TPU T_g. However, the fitted K value, K_{fit}, was found to *decrease* with increasing T_g of the POSS TPU (Table 1). The discrepancy between the K_{fit} and K_{G-T} indicates that specific interactions between the paclitaxel and the POSS TPUs must affect the T_g dependence of the blends. Indeed, Prud'homme et al.[40,41] proposed that the fitted K value from eq 1 could be used as a semiquantitative measure of the strength of intermolecular interactions between the blend components. Interestingly, Figure 5 shows that K_{fit} increases with PEG content in the POSS TPUs. The more PEG content in the POSS TPU, the higher K_{fit}, the stronger T_g dependence on paclitaxel, and, apparently, the more molecular stiffening by paclitaxel there is. This implies that PEG has stronger interaction with paclitaxel than LA and CL repeat units in the POSS TPUs, which will be further confirmed by the red shift of hydroxyl stretching peaks in the FTIR spectra.

The glass transition breadth, which is another indicator of the miscibility of the blends, was determined from the

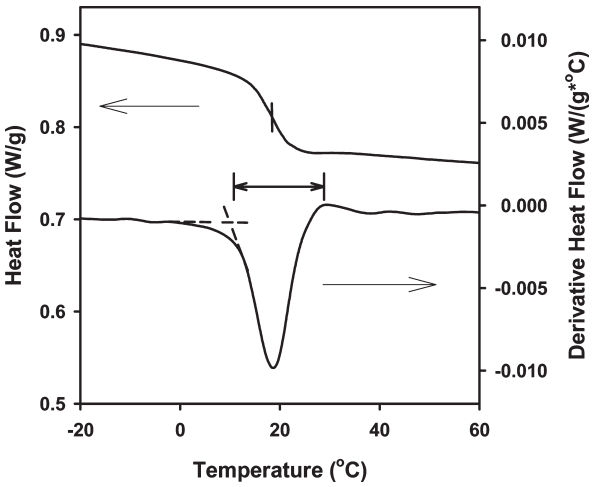

Figure 6. DSC second heating curve (above) and corresponding derivative of the DSC heating curve (below) of $[P_{1k}LA_{90}CL_{10}]$-$[LP]_3$ for the determination of the T_g breadth of the POSS TPU. The vertical bar in the heating curve indicates the T_g of the POSS TPU.

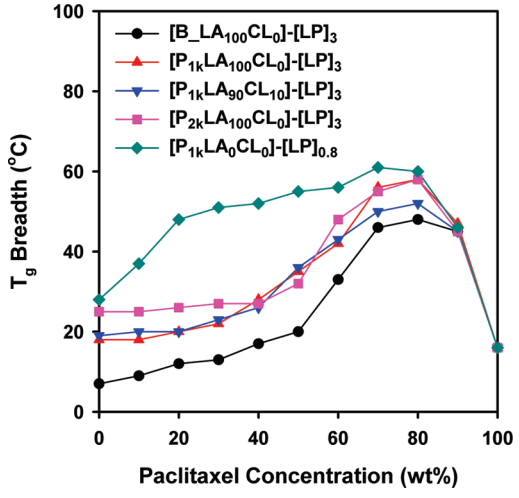

Figure 7. T_g breadth vs paclitaxel concentration for the PTx/POSS TPU blends.

derivative of the second heating curve obtained by DSC as described previously.[42−45] The determination of the T_g breadth of $[P_{1k}LA_{90}CL_{10}]$-$[LP]_3$ is illustrated in Figure 6. In the derivative heat flow curve, the onset of the glass transition is taken as crossing point from the extension lines of the baseline and the glass transition valley. The end point of the glass transition is obtained either using the same method as the onset of glass transition or using the temperature at the highest value of derivative heat flow if an aging peak appears at the end of the glass transition.

Figure 3b reveals the derivative heat flow curves of PTx/$[P_{1k}LA_{90}CL_{10}]$-$[LP]_3$ blends corresponding to the heat flow curves in Figure 3a. The T_g breadth of these blends does not change significantly for paclitaxel concentrations lower than 50 wt %, but increases quickly with further increment of the drug concentration, and then finally decreases when the drug concentration is close to 100 wt %. The dependences of T_g breadth vs the paclitaxel concentration of all PTx/POSS TPU blends are compiled in Figure 7. Clearly, all of the POSS TPUs except $[P_{1k}LA_0CL_0]$-$[LP]_{0.8}$ exhibits the same trend as $[P_{1k}LA_{90}CL_{10}]$-$[LP]_3$. In $[P_{1k}LA_0CL_0]$-$[LP]_{0.8}$, the T_g breadth increases significantly for all proportions even with 10 wt % incorporation of the paclitaxel. These results

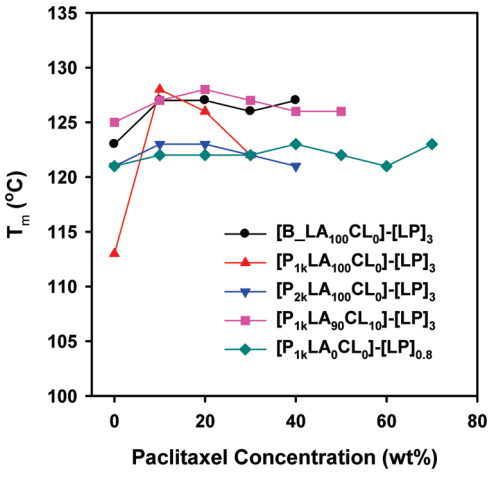

Figure 8. Paclitaxel concentration dependence of T_m of the PTx/POSS TPU blends obtained from their DSC second heating curves.

indicate that partial phase separation is possible in the PTx/POSS TPU blends at high paclitaxel concentrations, especially for the PTx/$[P_{1k}LA_0CL_0]$-$[LP]_{0.8}$ blends. On the other hand, for paclitaxel concentrations lower than 50 wt %, the POSS TPUs, except PTx/$[P_{1k}LA_0CL_0]$-$[LP]_{0.8}$, with higher PEG content show more stable T_g breadth with increasing drug concentration. This indicates that strong interactions between PEG and paclitaxel promote miscibility between the drug and the polymer. Interestingly, compared to $[P_{1k}LA_0CL_0]$-$[LP]_{0.8}$ containing pure PEG in the soft segment, $[B\_LA_{100}CL_0]$-$[LP]_3$ employs pure LA repeat units in the soft segment and exhibits even more favorable miscibility with paclitaxel. This indicates that, despite the strong interactions of the PEG with paclitaxel, the more hydrophobic components of the LA/CL repeat units in the polyurethanes are still required for the molecular-level miscibility with the drug, which will be further discussed later.

Continuing, the melting peaks in the DSC second heating curves of the PTx/POSS TPU blends were analyzed and compared. As shown in Figure 8, the incorporation of the paclitaxel in the POSS TPU blends slightly increases the blend T_m. According to the Flory−Huggins theory,[46] a melting temperature increase indicates a comparably unfavorable interaction between components, in this case, the drug and POSS. Considering this theory, the addition of paclitaxel drives stronger phase separation of the POSS hard segment from the amorphous phase in POSS TPUs, leading to enhanced POSS crystallization. As shown in Figure 9, the melting enthalpy of PTx/POSS TPU blends, normalized by the polymer mass ($\Delta H_{m,POSS\,TPU}$), first increases with paclitaxel concentration and then drops greatly to the point where the melting peaks cannot be detected. When the paclitaxel concentration is higher than 70 wt % for $[P_{1k}LA_0CL_0]$-$[LP]_{0.8}$ or 40−50 wt % for other POSS TPUs, no melting peak was detected in the DSC traces and the PTx/POSS TPU films were found to be very brittle. The higher paclitaxel concentration in $[P_{1k}LA_0CL_0]$-$[LP]_{0.8}$ than other POSS TPUs without loss of the mechanical strength can be explained by the much higher POSS content in this polymer (Table 1).

Specific Interactions. The specific interactions in the PTx/POSS TPU blends, as indicated in the K_{fit} derived from the Gordon−Taylor equation, were further investigated and confirmed using FTIR. Figure 10 shows the FTIR spectra of the PTx/$[B\_LA_{100}CL_0]$-$[LP]_3$ blends—as a representative set—with the increment of 20 wt % in the paclitaxel concentration. The peak at 711 cm^{-1} is assigned to the out-of-plane deformation of the C−H in the phenyl ring in

the paclitaxel since only the drug contains phenyl rings. Clearly, this peak does not appear in the spectrum of [B_LA$_{100}$CL$_0$]-[LP]$_3$ but increases in intensity gradually with increasing drug concentration. On the other hand, the peak intensity in the hydroxyl stretching region from 3100 to 3700 cm^{-1} is negligible in the pure POSS TPU but increases rapidly with paclitaxel concentration. This is due to paclitaxel's four H-bonding donors (Scheme 1) but also may come from the dilute H-bonding donors (N−H) in the urethane linkers of the POSS TPU (Scheme 2). Similar results as [B_LA$_{100}$CL$_0$]-[LP]$_3$ were observed in all the other POSS TPUs except [P$_{1k}$LA$_0$CL$_0$]-[LP]$_{0.8}$ (see Supporting Information for FTIR spectra). [P$_{1k}$LA$_0$CL$_0$]-[LP]$_{0.8}$ contains a much higher concentration of urethane linkers than the other POSS TPUs and demonstrates significant peaks in this spectral region, 3100−3700 cm^{-1}.

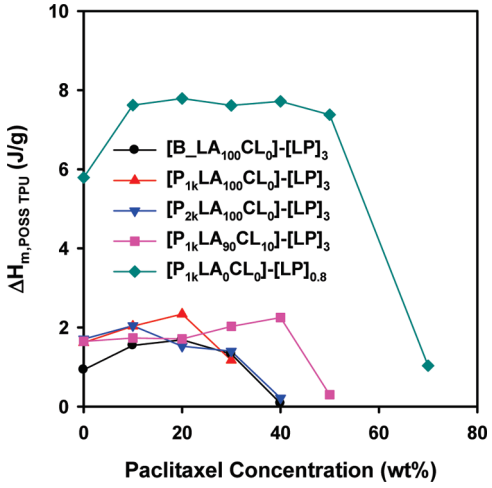

Figure 9. Paclitaxel concentration dependence of the melting enthalpy of the PTx/POSS TPU blends normalized by the POSS TPU mass, $\Delta H_{m,POSS\ TPU}$, obtained from their DSC second heating curves.

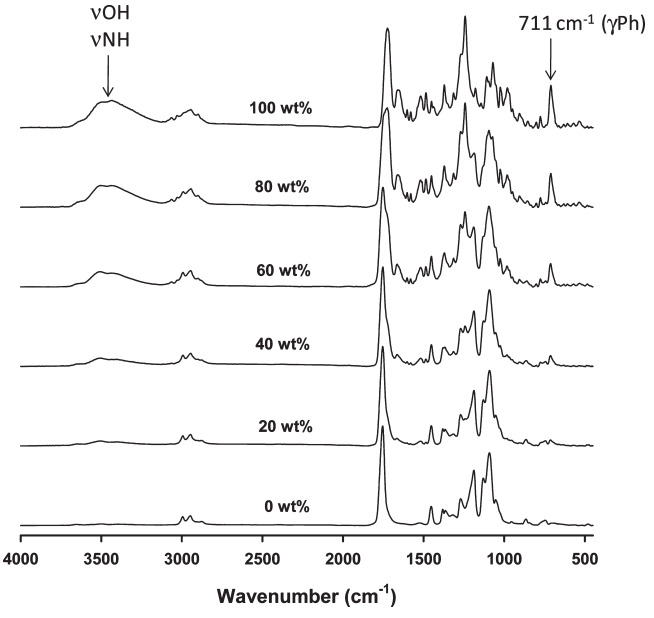

Figure 10. FTIR spectra of the PTx/[B_LA$_{100}$CL$_0$]-[LP]$_3$ blends with the paclitaxel weight percentage indicated above each curve.

Next, we compared the same spectral region of the three POSS TPU blends, including [B_LA$_{100}$CL$_0$]-[LP]$_3$, [P$_{1k}$LA$_{100}$CL$_0$]-[LP]$_3$, and [P$_{2k}$LA$_{100}$CL$_0$]-[LP]$_3$, with normalization by the OH dimer peak at 3506 cm^{-1}.[47] Interestingly, Figure 11 shows a red shift of the hydroxyl stretching region around 3400 cm^{-1} as the PEG content increases from 0 wt % in [B_LA$_{100}$CL$_0$]-[LP]$_3$, to 7 wt % in [P$_{1k}$LA$_{100}$CL$_0$]-[LP]$_3$, and finally to 14 wt % in [P$_{2k}$LA$_{100}$CL$_0$]-[LP]$_3$. Furthermore, a new shoulder peak around 3300 cm^{-1} assigned to −OH multimers first appears in the shoulder of the spectrum of PTx/[P$_{1k}$LA$_{100}$CL$_0$]-[LP]$_3$ blends with the paclitaxel concentration of 20 wt % and then becomes very strong in PTx/[P$_{2k}$LA$_{100}$CL$_0$]-[LP]$_3$ blends with the paclitaxel concentration from 20 to 60 wt %. Similar results as [P$_{1k}$LA$_{100}$CL$_0$]-[LP]$_3$ were observed in [P$_{1k}$LA$_{90}$CL$_{10}$]-[LP]$_3$ with the same PEG content (see Supporting Information for the FTIR spectra in the hydroxyl stretching region). In these four blends, the majority of H-bonding donors are due to the paclitaxel, and therefore competitive interactions are expected to exist between PTx/PTx, in PTx/LA or CL repeat units, and in PTx/PEG. The appearance of the new shoulder peak in the lower wavenumber region of the hydroxyl stretching range suggests that the large concentration of oxygen atoms (H-bond acceptors) in PEG enables the formation of −OH multimers and stronger H-bonding interactions with paclitaxel than the LA/CL repeat units in the POSS TPUs. Additionally, the strong interactions of the PEG and the paclitaxel cause a decrease in the intensity of the weak peak/shoulder at 3650 cm^{-1}, which is assigned to free −OH group, with increasing PEG content in the POSS TPUs for the blends at the same drug concentration. These results are consistent with the favorable interactions between paclitaxel and PEG in the PTx/PLGA/PEG blends reported by Kang et al.[27] Nevertheless, as mentioned above, the pure PEG employed in the soft segment of [P$_{1k}$LA$_0$CL$_0$]-[LP]$_{0.8}$ exhibits even less favorable miscibility with paclitaxel than the pure LA repeat units used in the soft segment of [B_LA$_{100}$CL$_0$]-[LP]$_3$. This is probably due to the LA repeat unit not only providing oxygens in its ester bond as H-bonding acceptor for paclitaxel, but also being more hydrophobic

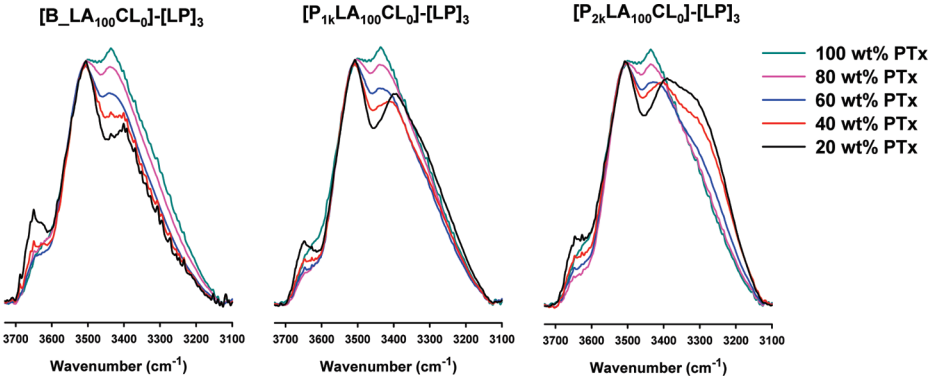

Figure 11. FTIR spectra in the hydroxyl stretching region of the PTx/POSS TPU blends.

and so more compatible with the hydrophobic part of the drug (Scheme 1) compared to the PEG segment.

Conclusions

There is always a need for new biodegradable or biostable biomedical systems with controlled and tailored properties for various applications, including drug-delivery systems, tissue-engineered bioscaffolds, and green biomaterials. Nevertheless, very few studies have provided systematically fundamental investigation of solid-state characteristics of drug-delivery polymeric systems. The incorporation of drug into polymeric systems, especially at high drug concentrations, can not only affect the polymer properties of the systems, but also influence the release mechanisms and therapeutic efficiencies of the drug. Furthermore, the understanding of these small molecule−polymer systems contributes greatly for developing other polymeric systems of desired properties.

Excellent miscibility of paclitaxel in a family of polymers over the whole range of the drug concentration was reported for the first time. Systematic investigations of the PTx/POSS TPU blends reveal that paclitaxel is not only amorphous in the polyurethanes, but also serves as an antiplasticizer and clearly exhibits strong H-bonding interactions with the PEG segments in the polymers. Favorable interactions between the paclitaxel with the LA/CL repeat units in the POSS TPUs were confirmed by their miscibility at all the proportions of the drug concentration, whereas unfavorable interactions between the drug and the POSS were indicated by the effect of the incorporation of the paclitaxel on the melting behavior of the POSS in the polymers. The comparably stable POSS crystallization in these blends shows great potential for the drug-loaded polymeric systems requiring high mechanical strength in processing and during drug release.[10,48] Compared to $[P_{1k}LA_{100}CL_0]$-$[LP]_3$, no significant difference were observed from $[P_{1k}LA_{90}CL_{10}]$-$[LP]_3$ in terms of the morphology, miscibility, and specific interactions with the paclitaxel. The addition of CL repeat units in the POSS TPUs can be utilized conveniently to modulate the polymer mechanical properties (e.g., lower polymer T_g) and the polymer degradation behavior. We contend that investigations into the morphology, miscibility, and specific interactions of the PTx/POSS TPU blends can be helpful not only for designing various polymeric formations with high drug-loading and high therapeutic efficiency, but also for those in biomedical applications with strict mechanical requirements.

Interestingly, the presence of −OH multimers supports the strong specific interactions between paclitaxel and PEG in the drug/POSS TPU blends, but the PEG H-bonding is not necessary for the drug miscibility in these systems. We observed that the POSS-based TPU without PEG also exhibited excellent miscibility with paclitaxel. In addition, the POSS-based TPU with soft segment of pure PEG even demonstrated less miscibility with the drug than the TPU without PEG. Moreover, the TPU containing significant amount of LA repeat unit showed higher drug miscibility with higher PEG content. Therefore, the most favorable interactions were observed for $[P_{2k}LA_{100}CL_0]$-$[LP]_3$ which contained 14 wt % PEG and 64 wt % LA repeat units. In contrast, the miscibility with paclitaxel in $[P_{1k}LA_0CL_0]$-$[LP]_{0.8}$ using pure PEG as the soft segment is even less than $[B\_LA_{100}CL_0]$-$[LP]_3$ consisting of pure LA repeat units in the soft segment. Too high PEG content in the polymer apparently disrupts molecular miscibility with the drug, which is probably due to both hydrophobic and hydrophilic functional groups existing in the paclitaxel structure. When the polymer soft segment is comparably hydrophobic, the H-bonding interactions can promote the favorable interactions between the drug and the POSS-based TPUs. Considering the limited choices of antiplasticizer for polymeric systems, this interesting finding may be helpful to design antiplasticizer/plasticizer for general polymer materials, and provide useful information to adjust the properties of the polymeric systems.

Acknowledgment. The authors thank Boston Scientific Corp. for the financial support of this work and Professor Jeremy L. Gilbert at Syracuse University for generously providing the usage of the FTIR.

Supporting Information Available: WAXD, DSC second heating curves and corresponding derivatives of the DSC heating curves, and FTIR spectra of PTx/POSS TPU blends. This material is available free of charge via the Internet at http://pubs.acs.org.

References and Notes

(1) Hancock, B. C.; Zografi, G. *J. Pharm. Sci.* **1997**, *86*, 1–12.
(2) Hancock, B. C.; Parks, M. *Pharm. Res.* **2000**, *17*, 397–404.
(3) Fakes, M. G.; Vakkalagadda, B. J.; Qian, F.; Desikan, S.; Gandhi, R. B.; Lai, C.; Hsieh, A.; Franchini, M. K.; Toale, H.; Brown, J. *Int. J. Pharm.* **2009**, *370*, 167–174.
(4) Spencer, C. M.; Faulds, D. *Drugs* **1994**, *48*, 794–847.
(5) Grube, E.; Silber, S.; Hauptmann, K. E.; Mueller, R.; Buellesfeld, L.; Gerckens, U.; Russell, M. E. *Circulation* **2003**, *107* (1), 38–42.
(6) Liggins, R. T.; Hunter, W. L.; Burt, H. M. *J. Pharm. Sci.* **1997**, *86*, 1458–1463.
(7) Dordunoo, S. K.; Burt, H. M. *Int. J. Pharm.* **1996**, *133* (1−2), 191–201.
(8) Cho, J. C.; Cheng, G. L.; Feng, D. S.; Faust, R.; Richard, R.; Schwarz, M.; Chan, K.; Boden, M. *Biomacromolecules* **2006**, *7* (11), 2997–3007.
(9) Hanefeld, P.; Westedt, U.; Wombacher, R.; Kissel, T.; Schaper, A.; Wendorff, J. H.; Greiner, A. *Biomacromolecules* **2006**, *7* (7), 2086–2090.
(10) Guo, Q.; Knight, P. T.; Mather, P. T. *J. Controlled Release* **2009**, *137*, 224–233.
(11) Sharma, A.; Mayhew, E.; Bolcsak, L.; Cavanaugh, C.; Harmon, P.; Janoff, A.; Bernacki, R. J. *Int. J. Cancer* **1997**, *71*, 103–107.
(12) Crosasso, P.; Ceruti, M.; Brusa, P.; Arpicco, S.; Dosio, F.; Cattel, L. *J. Controlled Release* **2000**, *63*, 19–30.
(13) Straubinger, R. M.; Balasubramanian, S. V. *Methods Enzymol.* **2005**, *391*, 97–117.
(14) Liggins, R. T.; Burt, H. M. *Adv. Drug Delivery Rev.* **2002**, *54*, 191–202.
(15) Shuai, X. T.; Merdan, T.; Schaper, A. K.; Xi, F.; Kissel, T. *Bioconjugate Chem.* **2004**, *15*, 441–448.
(16) Lee, S. C.; Huh, K. M.; Lee, J.; Cho, Y. W.; Galinsky, R. E.; Park, K. *Biomacromolecules* **2007**, *8*, 202–208.
(17) Kim, S. Y.; Lee, Y. M. *Biomaterials* **2001**, *22*, 1697–1704.
(18) Feng, S. S.; Mu, L.; Win, K. Y.; Huang, G. F. *Curr. Med. Chem.* **2004**, *11*, 413–424.
(19) Elkharraz, K.; Faisant, N.; Guse, C.; Siepmann, F.; Arica-Yegin, B.; Oger, J. M.; Gust, R.; Goepferich, A.; Benoit, J. P.; Siepmann, J. *Int. J. Pharm.* **2006**, *314*, 127–136.
(20) Zhang, X.; Jackson, J. K.; Burt, H. M. *Int. J. Pharm.* **1996**, *132*, 195–206.
(21) Dhanikula, A. B.; Panchagnula, R. *AAPS J.* **2004**, *6*, e27.
(22) Lee, J. H.; Gi, U.-S.; Kim, J.-H.; Kim, Y.; Kim, S.-H.; Oh, H.; Min, B. *Bull. Korean Chem. Soc.* **2001**, *22*, 925–928.
(23) Richard, R. E.; Schwarz, M.; Ranade, S.; Chan, A. K.; Matyjaszewski, K.; Sumerlin, B. *Biomacromolecules* **2005**, *6*, 3410–3418.
(24) Westedt, U.; Wittmar, M.; Hellwig, M.; Hanefeld, P.; Greiner, A.; Schaper, A. K.; Kissel, T. *J. Controlled Release* **2006**, *111* (1−2), 235–246.
(25) Lionzo, M. I.; Ré, M. I.; Guterres, S. S.; Pohlmann, A. R. *J. Microencapsulation* **2007**, *24*, 175–186.
(26) Chokshi, R. J.; Sandhu, H. K.; Iyer, R. M.; Shah, N. H.; Malick, A. W.; Zia, H. *J. Pharm. Sci.* **2005**, *94*, 2463–2474.
(27) Kang, E.; Robinson, J.; Park, K.; Cheng, J. X. *J. Controlled Release* **2007**, *122*, 261–268.
(28) Knight, P. T.; Lee, K.; Qin, H.; Mather, P. T. *Biomacromolecules* **2008**, *9*, 2458–2467.
(29) Waddon, A. J.; Coughlin, E. B. *Chem. Mater.* **2003**, *15*, 4555–4561.
(30) Woo, E. M.; Mandal, T. K.; Chang, L. L.; Lee, S. C. *Polymer* **2000**, *41*, 6663–6670.
(31) Gordon, M.; Taylor, J. S. *J. Appl. Chem.* **1952**, *2*, 493–500.

(32) Zhang, G. B.; Zhang, J. M.; Wang, S. G.; Shen, D. Y. *J. Polym. Sci., Part B: Polym. Phys*. **2003**, *41*, 23–30.
(33) Forster, A.; Hempenstall, J.; Tucker; Rades, T. *Drug Dev. Ind. Pharm*. **2001**, *27*, 549–60.
(34) Nair, R.; Nyamweya, N.; Gonen, S.; Martinez-Miranda, L. J.; Hoag, S. W. *Int. J. Pharm*. **2001**, *225*, 83–96.
(35) Lodge, T. P.; McLeish, T. C. B. *Macromolecules* **2000**, *33*, 5278–5284.
(36) Kant, R.; Kumar, S. K.; Colby, R. H. *Macromolecules* **2003**, *36*, 10087–10094.
(37) Besancon, B. M.; Soles, C. L.; Green, P. F. *Phys. Rev. Lett*. **2006**, *97*, 057801.
(38) Schneider, H. A. *Makromol. Chem*. **1987**, *189*, 1941–1955.
(39) Simha, R.; Boyer, R. F. *J. Chem. Phys*. **1962**, *37*, 1003–1007.
(40) Belorgey, G.; Aubin, M.; Prud'homme, R. E. *Polymer* **1982**, *23*, 1051–1056.
(41) Belorgey, G.; Prud'homme, R. E. *J. Polym. Sci., Polym. Phys. Ed*. **1982**, *20*, 191–203.
(42) Song, M.; Hammiche, A.; Pollock, H. M.; Houston, D. J.; Reading, M. *Polymer* **1996**, *31*, 5661–5665.
(43) Hourston, D. J.; Song, M.; Hammiche, A.; Pollock, H. M.; Reading, M. *Polymer* **1997**, *38*, 1–7.
(44) Kim, J.; Mok, M. M.; Sandoval, R. W.; Woo, D. J.; Torkelson, J. M. *Macromolecules* **2006**, *39*, 6152–6160.
(45) Wong, C. L. H.; Kim, J.; Torkelson, J. M. *J. Polym. Sci., Part B: Polym. Phys*. **2007**, *45*, 2842–2849.
(46) Flory, P. J. *Principles of Polymer, Chemistry*; Cornell University Press; Ithaca, NY, 1953.
(47) Coleman, M. M.; Graf, J. F.; Painter, P. C. *Specific Interactions and the Miscibility of Polymer Blends*; Technomic Publishing Co., Inc.: Lancaster, PA, 1991.
(48) Wu, J.; Mather, P. T. *Polym. Rev*. **2009**, *49*, 25–63.